Hindawi
Mathematical Problems in Engineering
Volume 2022, Article ID 6452253, 9 pages
https://doi.org/10.1155/2022/6452253

Research Article

Numerical Simulation of Vapor-Liquid Two-Phase Saturated Steam Fluent Flow and Atomizing Jet Cleaning

Feng Yan[1] **and Yehua Pi**[2]

[1]*School of Mechanical Engineering, Hunan Mechatronics Vocational and Technical College, Changsha 410151, Hunan, China*
[2]*Research and Development Department of Hunan AVIC Precision Limited Company, Changsha 410200, Hunan, China*

Correspondence should be addressed to Feng Yan; yanfengkyzy@163.com

Received 24 February 2022; Accepted 28 March 2022; Published 19 April 2022

Academic Editor: Zaoli Yang

In order to reduce the serious impact of polluting particles on the performance and quality of high-precision machinery and equipment, a cleaning system that uses saturated steam to clean the surface of parts and components is designed to achieve high cleanliness requirements. Based on the standard k-ε model, the large-scale fluid simulation software ANSYS is used to simulate the flow pattern of the steam nozzle to obtain the best distance for steam cleaning. According to the simulation results, a steam cleaning machine was developed and put into an automated cleaning production line to clean three different types of aviation parts. The residual masses of the parts were 0.1 mg, 0.1 mg, and 0.2 mg, and the maximum particle diameters were 549.461 μm, 275.464 μm, and 399.660 μm. The cleaning results show that the saturated steam cleaner can meet the cleaning requirements and get better surface quality parts after cleaning.

1. Introduction

Industrial cleaning means that industrial parts are contaminated by various pollutants such as liquids and solids during the production, use, and storage process. These pollutants are cleaned by physical, chemical, or mechanical means to make industrial products reach a certain level of cleanliness. For the cleaning of industrial parts, it mainly refers to the cleaning of cutting lubricating fluid and metal impurities on the surface of the parts before the product is assembled. Product cleanliness is an important part of it, which is related to product performance, quality, service life, and reliability. In particular, high-tech products have the characteristics of high performance, high reliability, high precision, high integration, and miniaturization. They are very sensitive to cleanliness, and tiny pollutants will have a serious impact on product performance and quality [1].

Aerospace, engineering machinery, medical equipment, and other mechanical equipment can operate normally and smoothly, which is closely related to the surface cleanliness of components and components of such equipment. During the processing and manufacturing of precision parts, particles such as cutting fluid and oil stains attached to the surface of the parts need to be cleaned before assembly. At present, the traditional industrial cleaning methods mainly include ultrasonic cleaning [2], laser cleaning [3], and high-pressure water jet cleaning [4]. The cleaning solvents used are often tap water, chemical solution, etc. Although these methods can play a certain cleaning effect on the surface cleanliness of parts, but because the cleaning method is hand-held, the secondary pollution of waste liquid after cleaning, the transportation of cleaning parts is completed manually, and the rust protection of cleaning parts cannot be well solved, it is a challenge to realize large-scale and automatic industrial cleaning.

In order to solve the abovementioned industrial cleaning needs and existing problems, based on the original cleaning technology, a cleaning system was designed that uses saturated steam to clean the surface of parts [5] (pressure is 10 MPa, temperature is 180°C, colorless, odorless, and noncorrosive dry gas) to achieve high cleanliness requirements.

Saturated steam through high-pressure scouring, high-temperature evaporation, stripping fixed-point positioning, the grinding parts of parts, channels, blind holes, thread undercut, cross holes, and other parts which are difficult to clean and easy to residual abrasive particles are targeted, scoured, and cleaned so as to achieve the effect of high cleanliness which is difficult to achieve by general methods. In order to improve the efficiency of steam utilization, the best nozzle shape and the effective distance of steam cleaning was determined and the flow field of saturated steam was simulated.

2. Mathematical Method and Calculation Model

Based on the large-scale general finite element analysis software ANSYS, which integrates the analysis of structure, fluid, electromagnetic field, sound field, and coupling field, the flow field of steam is analyzed. Because the flow field of steam is very complex, we only studied the flow field of single nozzle and determined the optimal nozzle shape according to the analysis of flow field [6]. Then, the influence of nozzle size on the flow field is studied to determine the optimal distance of saturated steam cleaning.

2.1. Basic Equation. The steam makes turbulent movement in the pipe and is ejected through the nozzle. With the transformation of vapor-liquid phase, it belongs to the vapor-liquid two-phase flow system. It should follow the laws of physical conservation. The flow process involves the laws of mass conservation, momentum conservation, and energy conservation. The specific equation is as follows:

(1) Mass conservation equation:

$$\frac{\alpha_\rho}{\alpha_t} + \operatorname{div}(\rho \vec{u}) = 0, \tag{1}$$

where ρ is the fluid density; t is the time, and $\vec{u}$ is the velocity vector.

(2) Momentum conservation equation:

$$\begin{aligned}
&\frac{\alpha(\rho u)}{\alpha_t} + \operatorname{div}(\rho u \vec{u}) = \operatorname{div}(\mu \operatorname{gradu}) - \frac{\alpha_p}{\alpha_x} + S_u,\\
&\frac{\alpha(\rho v)}{\alpha_t} + \operatorname{div}(\rho v \vec{u}) = \operatorname{div}(\mu \operatorname{gradv}) - \frac{\alpha_p}{\alpha_y} + S_v,\\
&\frac{\alpha(\rho w)}{\alpha_t} + \operatorname{div}(\rho w \vec{u}) = \operatorname{div}(\mu \operatorname{gradw}) - \frac{\alpha_p}{\alpha_z} + S_w,
\end{aligned} \tag{2}$$

where u is the dynamic viscosity and S_u, S_v, and S_w is the generalized source term of the momentum conservation equation.

(3) Energy conservation equation:

$$\frac{\alpha(\rho T)}{\alpha_t} + \operatorname{div}(\rho \vec{u} T) = \operatorname{div}\left(\frac{k}{c_p} \operatorname{grad} T\right) + S_T, \tag{3}$$

where T is the temperature, k is the thermal conductivity of the fluid, S_T is the viscous dissipation term, and c_p is the specific heat capacity.

2.2. Standard k-ε Model. Standard k-ε was first proposed by Launder and Spalding [7] in 1974. The stability and high accuracy of the model make it the most widely used model at present [8]. This model obtains the solutions of k and ε by solving the k equation of turbulent kinetic energy and the turbulent dissipation rate ε equation, then calculates the turbulent viscosity with the values of k and ε, and finally obtains the solution of Reynolds stress through Boussinesq hypothesis [9]. The effective viscosity coefficient μ_e is equal to the molecular viscosity coefficient μ plus the turbulent eddy viscosity coefficient μ_t as follows:

$$\mu_e = \mu + \mu_t. \tag{4}$$

In this equation,

$$\mu_t = \rho C_\mu \frac{k^2}{\varepsilon}. \tag{5}$$

Among them, ρ is the fluid density, C_μ is a constant term, and k is turbulent kinetic energy as follows:

$$k = \frac{\overline{u_i' u_i'}}{2}. \tag{6}$$

ε is the turbulent dissipation rate:

$$\varepsilon = \frac{\mu}{\rho}\left(\frac{\partial u_i'}{\partial x_j}\right) * \left(\frac{\partial u_i'}{\partial x_j}\right). \tag{7}$$

When fluid compression is not considered, the constraint equations for the turbulent kinetic energy k and the turbulent dissipation rate ε of the standard k-ε turbulence model are as follows:

$$\begin{aligned}
&\frac{\partial(\rho k)}{\partial t} + \frac{\partial\left(\rho k u_j\right)}{\partial x_j} = \frac{\partial}{\partial x_j}\left[\left(\mu + \frac{\mu_t}{\sigma_k}\right)\frac{\partial k}{\partial x_j}\right] + \rho(P_k - \varepsilon),\\
&\frac{\partial(\rho \varepsilon)}{\partial t} + \frac{\partial\left(\rho \varepsilon u_j\right)}{\partial x_j} = \frac{\partial}{\partial x_j}\left[\left(\mu + \frac{\mu_t}{\sigma_\varepsilon}\right)\frac{\partial \varepsilon}{\partial x_j}\right] + \rho \frac{\varepsilon}{k}(C_1 P_k - C_2 \varepsilon),
\end{aligned} \tag{8}$$

where

x_j is the coordinate component;

u_i and u_j are the average relative velocity components;

P_k is the term for the generation of turbulent kinetic energy, defined as

$$P_k = \frac{\mu_t}{\rho}\left(\frac{\partial u_i}{\partial x_j} + \frac{\partial u_j}{\partial x_i}\right)\frac{\partial u_i}{\partial u_j}. \tag{9}$$

In this model, the value of constant term is as follows: $C_\mu = 0.09$, $C_1 = 1.44$, $C_2 = 1.92$, $\sigma_k = 1.0$, and $\sigma_\varepsilon = 1.3$.

2.3. CFD Simulation Flow Field. CFD (computational fluid dynamics) simulation analysis of fluid dynamics is

equivalent to a virtual experiment on the computer, which can visually display and analyze the flow field and obtain various specific parameters in the flow process [10, 11]. At present, the mainstream solvers of CFD calculation include Fluent, CFX, air Pak, and STAR-CD in this subject; fluent solver is used to simulate the flow field of saturated steam nozzle. Fluent is a program used to solve liquid flow, heat conduction, and other fluid solid thermal coupling processes.

Fluent provides three two-phase flow models [12]: VOF model, mixture model, and Euler model. Because the VOF model adopts the average value for the physical parameters of each phase, when the velocity difference of each phase is large, it will affect the calculation results, so it is not suitable for the simulation of steam flow field. Eulerian model is the most complex multiphase flow model, and its solution accuracy is also the highest, but it is very difficult to converge in the iterative process, so it does not meet the calculation requirements. Therefore, the mixture model can be used to simulate multiphase flow with different velocities, which is widely used. Its continuity equation and momentum equation are as follows:

$$\begin{aligned} &\frac{\alpha_{\rho_1}}{\alpha_t} + \nabla(\rho_1 u) = 0, \\ &\frac{\alpha_{(\rho_1 u)}}{\alpha_t} + \nabla(\rho_1 u) = -\nabla p_1 + \nabla\tau + \nabla\int_{S(t)} \sigma k n \delta\left(x - x^{'}\right)\mathrm{d}S, \end{aligned} \tag{10}$$

where

t is time;

u is the speed;

σ is the surface tension coefficient of steam;

ρ_1 is density;

k is the steam conversion coefficient;

σ is the surface tension coefficient of steam;

p_1 is the pressure;

τ is shear stress;

n is the normal unit vector of surface s.

2.4. Boundary Condition Setting. Steam nozzle is a kind of fluid mechanical component for reducing pressure and increasing speed. In order to simplify the analysis, the thermodynamic model of the steam nozzle is assumed as follows: 1. The flow state of the fluid in the nozzle is one-dimensional steady-state flow. 2. The expansion and compression process of working steam is an isentropic process, ignoring the change of thermodynamic energy. In this way, the flow process of steam in the nozzle is the process of converting the enthalpy of steam into kinetic energy. The one-dimensional steady flow and constant entropy flow process are as follows:

$$\frac{d_p}{p} = -\kappa M^2 \frac{d_c}{c}, \tag{11}$$

where

p is the absolute pressure;

κ is the isentropic index;

M is Mach number; and

c is the speed.

To study the nozzle steam flow pattern, the main influence on the flow pattern change is the steam velocity, the calculation formula is as follows:

$$V_{ps} = \frac{Q_{ps}}{\rho_{ps} S}, \tag{12}$$

where V_{ps} is the steam flow rate, Q_{ps} is the steam flow rate, ρ_{ps} is the steam density, and S is the flow area of the nozzle.

According to the formula, when the steam flow rate is constant, reducing the flow area (or radius) of the nozzle can improve the steam injection speed and steam cleaning ability, but at the same time, it will also cause more serious noise problems due to the generation of supersonic flow shock wave. Therefore, the momentum value of inlet is 32 and the velocity magnitude is 510 m/s.

2.5. Model Building. Through the ANSYS software, the gas field analysis model is established, as shown in Figure 1. The air inlet is a single-hole cleaning gun to spray steam into the space, with a diameter of 5.6 mm; The cuboid represents the steam channel with a length of 300 mm. The outlet surface is the cross section of the steam flow channel, with the size of 150×150 mm.

2.6. Meshing. The model was imported into ANSYS for meshing, the steam inlet injection point and outlet plane of the model was defined, the air inlet was defined as an inlet, the outlet face as an outlet, and the remaining face as a restrictive wall that cannot pass steam. The efficiency and accuracy of numerical simulation calculation for flow problems mainly depend on the quality of grid generation and the algorithm used. Due to the complex flow field of the selected steam flow junction, the unstructured tetrahedral grid is used for division, as shown in Figure 2. The calculation area is discretized based on the finite volume method, the second-order implicit solution method is used to ensure the calculation accuracy, and the SIMPLEC algorithm based on the separation solver is selected for flow field coupling.

2.7. Iterative Convergence. In the finite element analysis, the implicit solution algorithm is used to solve the nonlinear problem. When the static balance equation is solved iteratively, it is easy to cause the calculation nonconvergence problem, so the initialization method is set to the initial state of miscellaneous (Hybrid), the number of iteration steps (number of iterations) is 500. The relationship between the residual value and the number of iteration steps is shown in Figure 3. From the figure, it can be seen that the vertical direction represents the size of the residual value. As the calculation proceeds,

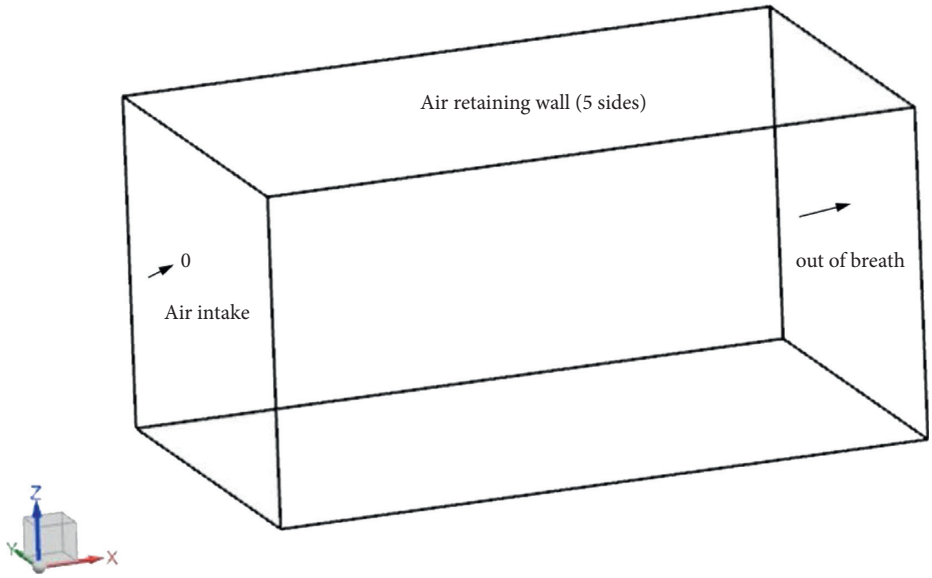

Figure 1: Gas field analysis model diagram.

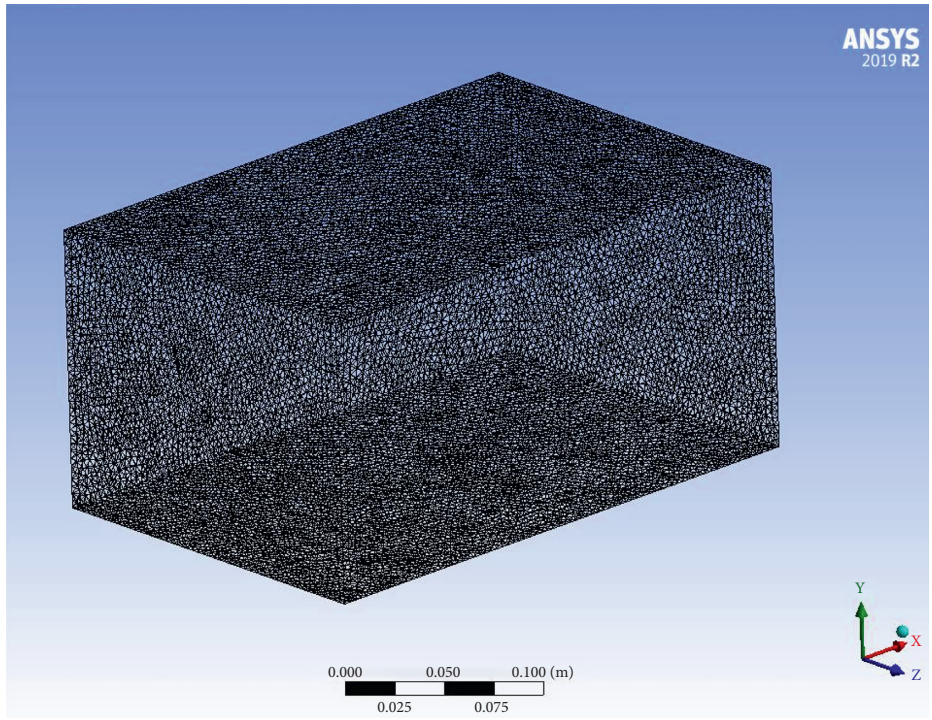

Figure 2: Grid of working model.

the value gradually decreases, indicating that the residual error is getting smaller and smaller and converging. The selected iteration method meet the needs of the solution.

3. Results and Discussion

By establishing a parameter model, the obtained steam flow field cloud diagram is shown in Figure 4, where the ordinate is the steam flow rate and the abscissa is the steam ejection distance.

It can be seen from the figure that the blue area is a static area, and there is no steam flowing through this area; The length of saturated steam flow in cyan and green areas is less than 120 mm, and the steam flow speed is faster. In the yellow and red regions, the length of the air flow is less than 20 mm, which is the supersonic region of saturated steam. In this region, the steam velocity is very fast, and shock wave (explosion wave and sound burst) phenomenon occurs. This kind of explosion can degrade and peel off any stubborn dirt and vaporize it. When the distance is beyond 120 mm, the

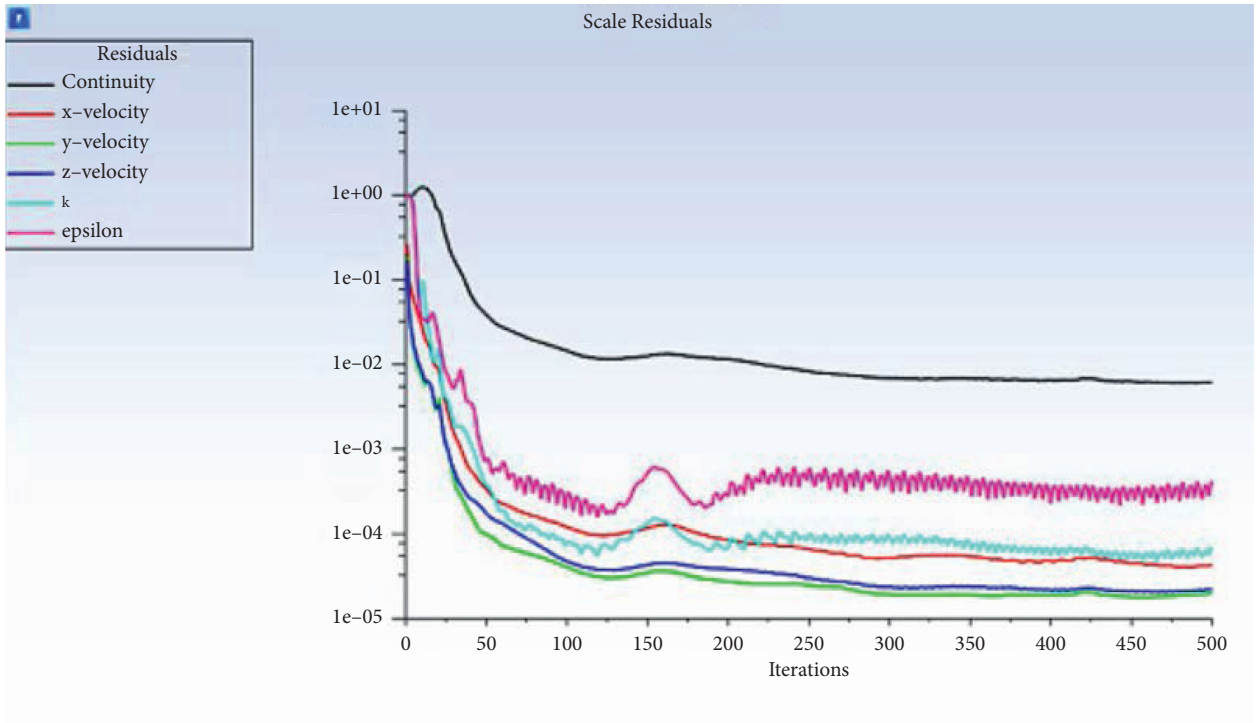

Figure 3: Residual error curve.

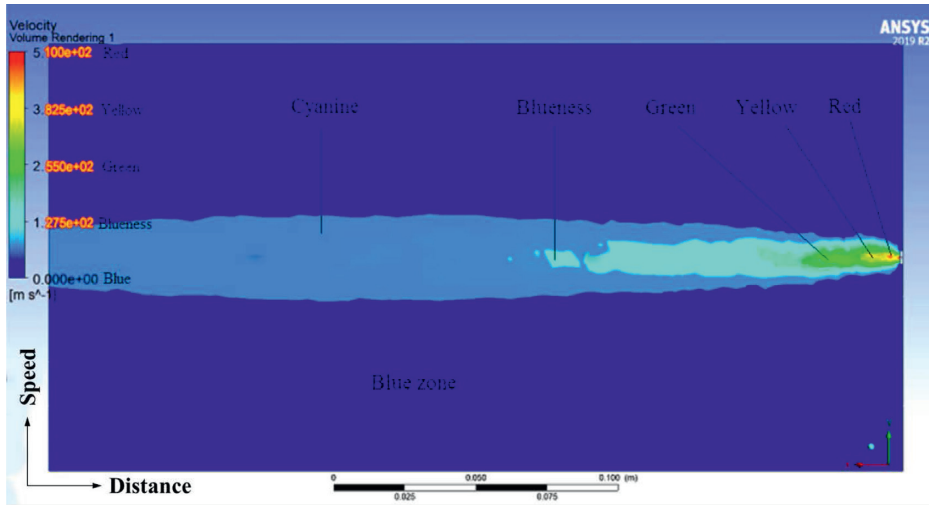

Figure 4: Cloud map of steam flow field.

velocity of steam flow slows down obviously and the ability of decontamination becomes worse. To sum up, the best distance of steam cleaning is the green red area, which has the best cleaning effect.

In the figure below, we have made some changes to the established model in order to obtain a better cleaning effect. The steam movement channel remains unchanged. The steam movement channel remains unchanged and is still a cuboid with a length of 300 mm. The size of the outlet section of the steam outflow is still 150 × 150 mm, and the aperture of the air inlet remains unchanged. The difference is that a single-sided 45-degree bell mouth angle is added at the entrance of the air intake. In the case of only changing the horn mouth angle, using the same parameter settings, through flow field analysis, the flow field diagram shown in Figure 5 is obtained.

From the figure above, we can see that the total length of steam flow is greatly shortened, and the steam velocity decays rapidly. This is not conducive to saturated steam to play its due cleaning capacity. This is consistent with the conclusion that the straight cylinder nozzle is better than the horn cone nozzle in saturated steam cleaning.

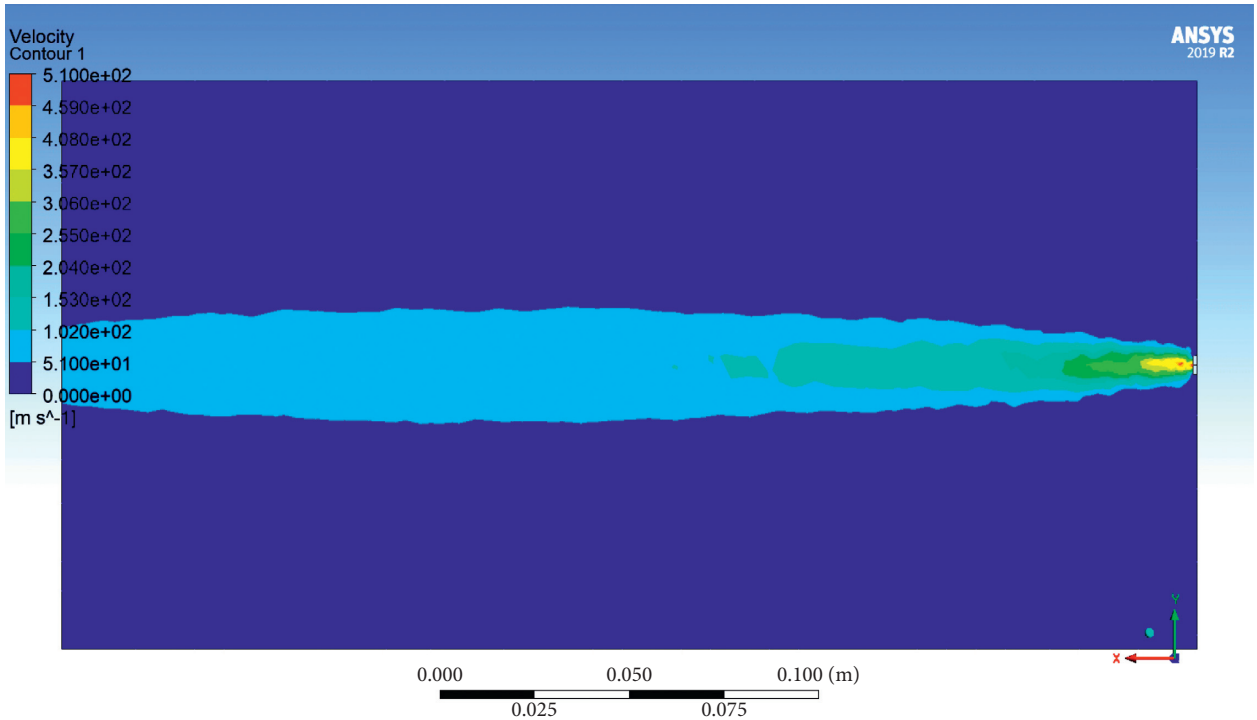

Figure 5: Cloud diagram of the steam flow field of the horn-shaped nozzle.

Figure 6: Saturated steam cleaning machine.

4. Particle Detection

Studies have shown that high-speed and relatively moving metal surfaces have more high-hard particles adhered to them, which will cause rapid and severe wear of these parts and greatly shorten their service life, such as aeroengine turbines, automobile engines, and high-power laser devices. Therefore, the cleanliness of the parts to be assembled is extremely important for improving the quality of the assembled products and prolonging the service life of the products.

Based on the simulation results of the nozzle steam pattern in the second chapter, we developed a saturated steam cleaning machine, as shown in Figure 6 and placed it in an automated cleaning production line, as shown in Figure 7. The process flow mainly includes: manual feeding, high-pressure chemical liquid water solvent spray cleaning, high-pressure air dewatering, high-temperature, and high-pressure saturated steam spraying, among which high-temperature and high-pressure saturated steam spraying is the main link.

Figure 7: Automated cleaning production line.

Figure 8: Olympus metallurgical microscope (GX71).

The particle contamination grade can be expressed by the size of the largest particle found. For precision grade cleaning, the wetted surface contaminant of 1000 cm is less than 1 mg (ISO 16232-2006).

The particle size distribution method is mainly used to calibrate the particle pollutants. The test method is to clean a certain number of parts under certain conditions, fully filter the cleaning solution through the filter membrane, collect the dirt on the surface of the filter membrane, then dry the filter membrane, detect with an electronic microscope, and count the dirt particles according to the particle size and quantity. The results of solid particle contamination of the measured parts can be obtained.

The aerospace parts processed by turning and milling include hole parts S190701, slot parts S190703, and blade parts S190705 (due to confidentiality involved, the parts diagram cannot be shown).

To test the cleanliness and particle size of cleaned aviation parts, Olympus metallographic microscope is used, as shown in Figure 8. The model number is gx71, which can be used for dark field, differential interference, and polarized light observation. The maximum magnification is 2000 times, and the minimum diameter is 1 μm. It can meet the needs of detection.

The test results of cleaned aviation parts are shown in Figure 9. The residual mass of parts s190701, s190703, and s190705 are 0.1 mg, 0.1 mg, and 0.2 mg, respectively, and the maximum particle diameters are 549.461 μm, 275.464 μm, 399.660 μm, respectively. The requirements of national standard and assembly requirements were met. Therefore, according to the simulation results of steam flow field, the designed saturated steam cleaning machine can meet the cleaning requirements and get better surface quality parts after cleaning.

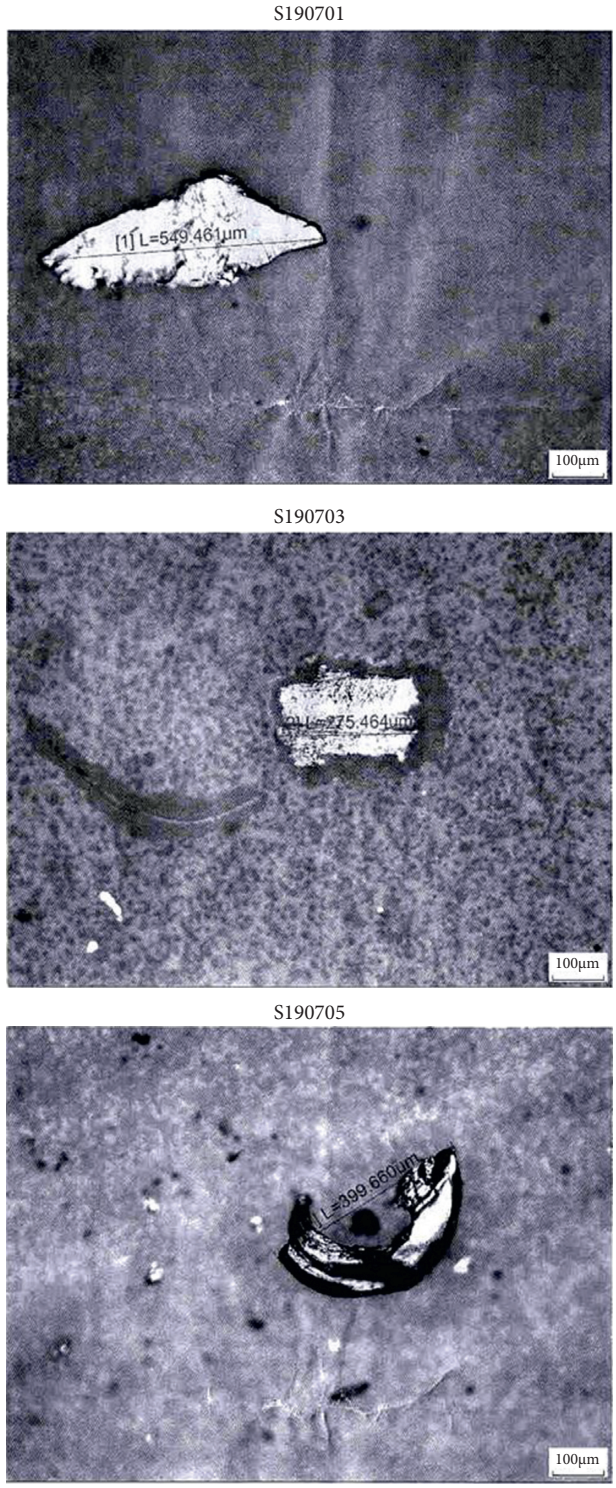

Figure 9: Inspection results of aviation parts.

5. Conclusion

Through the large-scale fluid simulation software ANSYS, the flow pattern of steam nozzle is simulated, and based on this, the saturated steam engine is developed and the automatic cleaning production line is designed, which solves the problem of serious quality and performance impact caused by the unclean cleaning of particles attached to the surface of aerospace, medical devices, and other precision equipment parts and provides a new idea for industrial cleaning.

Data Availability

The data supporting the findings of this study are available within the article.

Conflicts of Interest

The authors declare that they have no conflicts of interest.

Acknowledgments

This work was supported by the Hunan Province Innovation and Entrepreneurship Technology Investment Project (2017GK5032) and Hunan Province Science and Technology Innovation Platform and Talent Plan Project (2018TP2044).

References

[1] D. Essola, A. P. Njomoue, F. Offole, and P. N. Achille, "Low frequency vibratory cleaning of paint and rust contaminants from machines parts," *Proceedings of the Institution of Mechanical Engineers-Part B: Journal of Engineering Manufacture*, vol. 236, no. 41, Article ID 095440542110314, 2021.

[2] K. Ando, M. Sugawara, and R. Sakota, "Particle removal in ultrasonic water flow cleaning role of cavitation bubbles as cleaning agents," *Solid State Phenomena*, vol. 314, pp. 218–221, 2021.

[3] G. Lingyu, L. Yuqiang, G. Shaoning, W. Chunming, and J. Ping, "Numerical and experimental analysis for morphology evolution of 6061 aluminum alloy during nanosecond pulsed laser cleaning," *Surface and Coatings Technology*, vol. 432, 2022.

[4] D. Ning, Q. Wang, J. Tian et al., "Experimental study on the coating removing characteristics of high-pressure water jet by micro jet flow," *Micromachines*, vol. 12, no. 2, p. 173, 2021.

[5] D. Taler, P. Dzierwa, K. Kaczmarski, and T. Jan, "Optimisation of heating and cooling of pressure thick-walled components operating in the saturated steam area," *Energy*, vol. 231, p. 231, 2021.

[6] G. Wu, X. Zhao, D. Shi, and X. Wu, "Analysis of fluid-structure coupling vibration mechanism for subsea tree pipeline combined with fluent and ansys workbench," *Water*, vol. 13, no. 7, p. 955, 2021.

[7] B. E. Launder, "The numerical computations of turbulent flows," *Computer Methods in Applied Mechanics and Engineering*, vol. 3, 1974.

[8] N. H. Abu-Hamdeh, K. H. Almitani, A. A. Gari, and A. Ashkan, "FVM method based on K ε model to simulate the turbulent convection of nanofluid through the heat exchanger porous media," *Journal of Thermal Analysis and Calorimetry*, vol. 144, no. 10, 2021.

[9] R. S. Kartanegara and S. Sugianto, "Studi parametrik pemisahan energi aliran udara dalam tabung vorteks menggunakan model aliran viscous κ-ε," in *Proceedings of the Seminar Nasional Teknik Mesin Politeknik Negeri Jakarta*, Depok, Indonesia, January 2021.

[10] K. Nidhul, A. K. Yadav, S. Anish, and U. C. Arunachala, "Thermo-hydraulic and exergetic performance of a cost-effective solar air heater: CFD and experimental study," *Renewable Energy*, vol. 184, p. 184, 2022.

[11] S. Liang, "Study on flow characteristics of rough undulating single fracture based on CFD," *Materials Science and Engineering Conference Series*, vol. 780, p. 6, 2020.

[12] F. Costa, F. Mateus, and I. P. Júnior, "Optimization of hydrocyclon for phosphatic rock separation using CFD," *The Journal of Engineering and Exact Sciences*, vol. 7, no. 3, 2021.